行政院國家科學委員會專題研究計畫　成果報告

磯松素和血根鹼對人類乳癌細胞增生抑制作用和細胞程式死亡機制之探討

計畫類別：個別型計畫
計畫編號：NSC94-2320-B-041-007-
執行期間：94 年 08 月 01 日至 95 年 07 月 31 日
執行單位：嘉南藥理科技大學生物科技系(所)

計畫主持人：郭柏麟
共同主持人：林俊清
計畫參與人員：黃郁婷

報告類型：精簡報告

處理方式：本計畫涉及專利或其他智慧財產權，2 年後可公開查詢

中　華　民　國 95 年 10 月 26 日

行政院國家科學委員會專題研究計畫 成果報告

磯松素和血根碱對人類乳癌細胞增生抑制作用和細胞程式死亡機制之探討

計畫類別：個別型計畫
計畫編號：NSC94－2320－B－041－007
執行期間：2005 年 08 月 01 日至 2006 年 07 月 31 日
計畫主持人：郭柏麟
共同主持人：林俊清
計畫參與人員：黃郁婷

成果報告類型：精簡報告

處理方式：本計劃暫不公開

執行單位：嘉南藥理科技大學生物科技系

中　華　民　國　95　年　10 月　26　日

行政院國家科學委員會專題研究計畫成果報告

磯松素和血根碱對人類乳癌細胞增生

抑制作用和細胞程式死亡機制之探討

計畫編號：NSC94－2320－B－041－007

執行期限： 94 年 08 月 01 日至 95 年 07 月 31 日

主持人：郭柏麟，嘉南藥理科技大學生物科技系

處理方式：本計劃暫不公開

中文摘要

本研究主要探討磯松素(plumbagin)的抗乳癌活性和相關分子機轉。結果發現磯松素會造成細胞週期停滯(cell cycle arrest)以及細胞自噬(autophagy)。磯松素促使細胞週期停滯於 G2/M 期主要透過增加 p21 表現、Chk2 活化以及降低 cyclin B1、cyclin A、cdc2 和 cdc25C 的表現。除此，磯松素還會透過增加 p21 和 Cdc2 的結合，以及增加 Chk2 的活化促使 Cdc2 和 Cdc25C 的磷酸化而抑制 Cdc2 的功能。在細胞死亡誘導方面，磯松素主要會誘導細胞進行細胞自噬，而非細胞凋亡。磯松素可藉由抑制 AKT 的活化以及相關下游分子，包括 mammalian target of rapamycin (mTOR)、forkhead transcription factors (FKHR)和 glycogen synthase kinase-3beta (GSK)，有效的阻斷 PI3K (phosphatidylinositol 3-kinase)/AKT 訊息傳遞。再者，mTOR 的數個下游分子，包括 p70 ribosomal protein S6 kinase (p70S6 kinase)和 4E-BP1 的磷酸化也都一併受到抑制。當細胞過度表現 AKT 時會抑制磯松素所造成的細胞自噬作用。相對的，當 AKT 表現受到抑制時會明顯增加磯松素所造成的細胞自噬作用，因此證明磯松素透過 AKT 的抑制作用促使啟動細胞自噬。除此，磯松素在裸鼠(nude mice)的研究也證實了其在 in vivo 的條件下仍然具有抑制乳癌細胞增生、啟動細胞自噬以及抑制 AKT 活化的能力。綜合以上結果，本研究證實磯松素可藉由抑制 PI3K/AKT/mTOR 路徑促使細胞停滯以及啟動細胞自噬。

關鍵詞：磯松素、細胞週期、細胞自噬、AKT、mTOR

Abstract

This study is the first to investigate the anticancer effect of plumbagin in human breast cancer cells. Plumbagin exhibited cell proliferation inhibition by inducing cells to undergo G2/M arrest and autophagic cell death. Blockade of the cell cycle was associated with increased p21/WAF1 expression and Chk2 activation, and reduced amounts of cyclinB1, cyclinA, Cdc2 and Cdc25C. Plumbagin also reduced Cdc2 function by increasing the association of p21/WAF1/Cdc2 complex and the levels of inactivated phospho-Cdc2 and phospho-Cdc25C by Chk2 activation. Plumbagin triggered autophagic cell death, but not, predominantly, apoptosis. Pretreatment of cells with autophagy inhibitor bafilomycin suppressed plumbagin-mediated cell death. We also found that plumbagin inhibited survival signaling through the PI3K (phosphatidylinositol 3-kinase)/AKT signaling pathway by blocking the activation of AKT and downstream targets, including the mammalian target of rapamycin (mTOR), forkhead transcription factors (FKHR) and glycogen synthase kinase-3beta (GSK). Phosphorylation of both of mTOR's downstream targets, p70 ribosomal protein S6 kinase (p70S6 kinase) and 4E-BP1, was also diminished. Overexpression of AKT by AKT cDNA transfection decreased plumbagin-mediated autophagic cell death, whereas reduction of AKT expression by siRNA potentiated plumbagin's effect, supporting inhibition of AKT beneficial to autophagy. Furthermore, suppression of AKT by plumbagin enhanced the activation of Chk2, resulting in increased inactive phosphorylation of Cdc25C and Cdc2. Further investigation revealed that plumbagin's inhibition of cell growth was also evident in a nude mice model. Taken together, these results imply a critical role for AKT inhibition in plumbagin-induced G2/M arrest and autophagy of human breast cancer cells.

Keywords: AKT; autophagy; cell cycle; mTOR; plumbagin

Plumbagin induces G2/M arrest and autophagy by inhibiting the AKT/mTOR pathway in breast cancer cells

Po-Lin Kuo,[1] Ya-Ling Hsu,[2] and Chien-Yu Cho[3]

[1]Cell Biology Laboratory, Department of Biotechnology and [2]Department of Pharmacy, Chia-Nan University of Pharmacy and Science, Tainan, Taiwan; [3]Graduate Institute of Natural Products, Kaohsiung Medical University, Kaohsiung, Taiwan

Requests for reprints: Po-Lin Kuo, Ph.D., Cell Biology Laboratory, Department of Biotechnology, Chia-Nan University of Pharmacy and Science, Tainan 717, Taiwan, Phone: 886-6-266-4911 ext. 520, Fax: 886-6-266-2135, E-mail: kuopolin@seed.net.tw

Running title: Plumbagin-mediated signaling in breast cancer

Keywords: AKT; autophagy; cell cycle; mTOR; plumbagin

Abbreviations: AVO, acidic vesicular organelles ; FKHR, forkhead transcription factors; MDC, monodansylcadaverine; mTOR, mammalian target of rapamycin; PI3K, phosphatidylinositol 3-kinase; p70S6 kinase, p70 ribosomal protein S6 kinase, siRNA, small interfering RNA; TUNEL, terminal deoxynucleotidyl transferase-mediated deoxyuridine triphosphate nick endlabeling.

Abstract

This study is the first to investigate the anticancer effect of plumbagin in human breast cancer cells. Plumbagin exhibited cell proliferation inhibition by inducing cells to undergo G2/M arrest and autophagic cell death. Blockade of the cell cycle was associated with increased p21/WAF1 expression and Chk2 activation, and reduced amounts of cyclinB1, cyclinA, Cdc2 and Cdc25C. Plumbagin also reduced Cdc2 function by increasing the association of p21/WAF1/Cdc2 complex and the levels of inactivated phospho-Cdc2 and phospho-Cdc25C by Chk2 activation. Plumbagin triggered autophagic cell death, but not, predominantly, apoptosis. Pretreatment of cells with autophagy inhibitor bafilomycin suppressed plumbagin-mediated cell death. We also found that plumbagin inhibited survival signaling through the PI3K (phosphatidylinositol 3-kinase)/AKT signaling pathway by blocking the activation of AKT and downstream targets, including the mammalian target of rapamycin (mTOR), forkhead transcription factors (FKHR) and glycogen synthase kinase-3beta (GSK). Phosphorylation of both of mTOR's downstream targets, p70 ribosomal protein S6 kinase (p70S6 kinase) and 4E-BP1, was also diminished. Overexpression of AKT by AKT cDNA transfection decreased plumbagin-mediated autophagic cell death, whereas reduction of AKT expression by siRNA potentiated plumbagin's effect, supporting inhibition of AKT beneficial to autophagy. Furthermore, suppression of AKT by plumbagin enhanced the activation of Chk2, resulting in increased inactive

phosphorylation of Cdc25C and Cdc2. Further investigation revealed that plumbagin's inhibition of cell growth was also evident in a nude mice model. Taken together, these results imply a critical role for AKT inhibition in plumbagin-induced G2/M arrest and autophagy of human breast cancer cells.

Introduction

Autophagic cell death is an important physiological process occurring in all eukaryotic cells (1, 2). The characterization of autophagic cell death is revealed by massive degradation of cellular contents, including portions of the cytoplasm and intracellular organelles, by means of complicated intracellular membrane/vesicle reorganization and lysosomal hydrolases (1-3). Autophagic cell death is involved in development and stress responses, and has been observed in several human diseases such as neurodegenerative disease, muscular disorders and pathogen resistance (2). Furthermore, like apoptosis, autophagic cell death is found to be suppressed in malignant tumors and involved in tumorigenesis. A number of studies have reported that autophagy is activated in response to γ-irradiation and various anticancer therapies (2, 4, 5). Several molecular and cell signaling pathways have been implicated in regulating autophagy, such as BECN1, DAPK (death-associated protein kinase), DRP1 (death-associated related protein kinase 1), MAPK (mitogen-activated kinase) and PI3K-AKT-mTOR (phosphatidylinositol 3-kinase/AKT/ mammalian target of rapamycin) pathways (1, 2, 6). However, detailed mechanisms of the autophagic cell signaling pathway are poorly understood.

PI3K/AKT signaling has been found to be involved in the survival and proliferation of a variety of tumor cells, including breast cancers (7, 8). Hyperactivation of PI3K/AKT has resulted in altering the response of tumor cells to

chemotherapy and irradiation (9, 10). PI3K is a heterodimer of the regulatory p85 and catalytic p110 subunits. A variety of growth factors can activate PI3K through activation of their cognate receptors, leading to the activation of AKT signaling. AKT mediates a variety of biological functions, including glucose uptake, protein synthesis, and inhibition of cell death (8). AKT can mediate cell survival and growth by regulating both post-translational mechanisms and gene transcription. AKT activity is regulated by phosphorylation on two regulatory residues, threonine 308 (Thr 308) in the activation loop of the catalytic domain and serine 473 (Ser 473) in the regulatory domain (8). Once activated, AKT can promote cell survival by inhibiting types Ⅰ (apoptosis) and Ⅱ (autophagy) cell death by phosphorylation of several signaling proteins, including cAMP-response-element-binding protein, mTOR proteins, forkhead transcription factors (FKHR) and glycogen synthase kinase-3 (GSK-3) (1, 2, 8, 11). mTOR is a serine-threonine kinase that regulates the function of transcriptional regulators p70 ribosomal protein S6 kinase (p70S6 kinase) and 4E-BP1 (8, 12). Recent studies have shown that the inhibition of AKT and its downtarget mTOR signaling contributes to the initiation of autophagy (11, 13). Therefore, mTOR signaling has emerged as an important and attractive therapeutic target for cancer therapy.

Eukaryotic cell cycle progression involves the sequential activation of Cdks,

whose activation is dependent upon their association with cyclins (14). The complex formed by the association of Cdc2 and cyclinB1 plays a major role at entry into mitosis (14). Regulation of Cdc2 activity is controlled at three levels. First, Cdc2 is inactive as a monomer and must bind with cyclinB during the G2/M transition (14, 15). Second, it is also regulated by cyclin-dependent kinase inhibitors (CKIs), such as p21/WAF1 and p27/KIP, binds to cyclin-CDK complexes and prevents kinase activation (14). Finally, a series of reversible phosphorylations regulates the activity of the Cdc2/cyclinB complex. Phosphorylation of Cdc2 on Thr 161 by Cdk-activating kinase (CAK) is essential for Cdc2 kinase activity (14). In contrast, Cdc2 is committed to inhibitory phosphorylation at Tyr 15 and Thr 14 by Wee1/Mik1/Myt1 kinases (14, 16). During the G2/M transition, Cdc2 is rapidly converted into the active form by Tyr15 dephosphorylation catalyzed by the Cdc25 phosphatase. In mammalian cells, Chk2 phosphorylated Cdc25C at Ser 216, a site known to be involved in negative regulation of Cdc25C (17). Phosphorylation of Cdc25C on Ser 216 interferes with Cdc25C's ability to promote mitotic entry (17). Thus, the activity of Chk2 exceeds that of Cdc25C in the G2/M phase, and this regulation is therefore crucial to the G2/M transition.

Plumbagin (5-hydroxy-2-methyl-1,4-naphthoquinone), a quinonoid constituent isolated from the root of *Plumbago zeylanica* L. (also known as "Chitrak"), has been

shown to exert anticarcinogenic, anti-atherosclerotic and antimicrobial effects (18-21). The root of *P. zeylanica* L has been used in Indian medicine for approximately 2,750 years and its component possess anti-atherogenic, cardiotonic, hepatoprotective, and neuroprotective properties (19). In short, plumbagin has exhibited anticancer and antiproliferation properties in a variety of cell lines and animal models (22, 23). In this study, we determined the cell growth inhibition activity of plumbagin by using *in vitro* and *in vivo* experimental models, and examined its effect on cell cycle distribution and autophagic cell death in two human breast cancer cell line, MDA-MB-231 and MCF-7. Furthermore, to establish plumbagin's anticancer mechanism, we assayed the levels of cell cycle control- and autophagy-related molecules, which are strongly associated with the cell death signal transduction pathway and affect the chemosensitivity of tumor cells to anticancer agents.

Materials and Methods

Materials

Fetal calf serum (FCS), RPMI 1640, penicillin G, streptomycin, and amphotericin B were obtained from GIBCO BRL (Gaithersburg, MD). Plumbagin, acridine orange, monodansylcadaverine (MDC), bafilomycin, dimethyl sulfoxide (DMSO), ribonuclease (RNase), trypsin-EDTA, and propidium iodide (PI) were purchased from

Sigma Chemical (St. Louis, MO). XTT was obtained from Roche Diagnostics GmbH (Germany). PI3K p85, PI3K 110α, 110γ, mTOR, phospho-mTOR, p70S6K, and phospho-p706SK antibodies, and AKT activity assay kit were obtained from Cell Signaling Technology (Beverly, MA). ATK cDNA plasmid was obtained from Upstate Biotechnology Inc. AKT1 siRNA and control siRNA were purchased from Ambion (Austin, TX). Beclin-1 siRNA was purchased from Dharmacon (Boulder, CO).

Cell culture

MCF-7 (ATCC HTB-22) and MDA-MD-231 cells (ATCC HTB-26) were obtained from the American Type Cell Culture Collection (Manassas, VA). MCF-7 cells were cultured in DMEM with nonessential amino acids, 0.1 mM sodium pyruvate, 10 μg/ml insulin, and 10% FCS. MDA-MB-231 cells were cultured in RPMI 1640 (Life Technologies, Inc., Grand Island, NY) supplemented with 10% FCS and 1% penicillin-streptomycin solution (Life Technologies, Inc.).

Cell proliferation and clonogenic assay

Inhibition of cell proliferation by plumbagin was measured by XTT (sodium 3'-[1-(phenylamino-carbonyl)-3,4-tetrazolium]-bis(4-methoxy-6-nitro) benzene-sulfonic acid hydrate) assay. Cells were plated in 96-well culture plates (1×10^4 cells/well). After 24 h incubation, the cells were treated with plumbagin (0, 2.5, 5, 10, and 20 μM) for 48 h. Fifty μl of XTT test solution, which was prepared by

mixing 5 ml of XTT-labeling reagent with 100 μl of electron coupling reagent, was then added to each well. The absorbance was measured on an ELISA reader (Multiskan EX, Labsystems) at a test wavelength of 492 nm and a reference wavelength of 690 nm. Data were calculated as the percentage of inhibition by the following formula: inhibition % = [100 - (ODt/ODs) × 100] %. ODt and ODs indicated the optical density of the test substances and the solvent control, respectively

To determine long-term effects, cells were treated with plumbagin at various concentrations for 1 h. After being rinsed with fresh medium, cells were allowed to grow for 14 days to form colonies which were then stained with crystal violet (0.4 g/L; Sigma). Clonogenic assay was used to elucidate the possible differences in long-term effects of plumbagin on human breast cells.

Cell cycle analysis

To determine cell cycle distribution analysis, 5×10^5 cells were plated in 60mm dishes and treated with plumbagin (0, 4, and 8 μM) for 6 h. After treatment, the cells were collected by trypsinization, fixed in 70% ethanol, washed in phosphate-buffered saline (PBS), resuspended in 1 ml of PBS containing 1 mg/ml RNase and 50 μg/ml propidium iodide, incubated in the dark for 30 min at room temperature, and analyzed by EPICS flow cytometer. The data were analyzed using Multicycle software

(Phoenix Flow Systems, San Diego, CA).

Apoptosis assay

Cells (1×10^6) were treated with vehicle alone (0.1% DMSO) and various concentrations of plumbagin and cisplatin for 48 h, then collected by centrifugation. Pellets were lysed by DNA lysis buffer (10 mM Tris, pH 7.5, 400 mM EDTA, and 1% Triton X-100) then centrifuged. The supernatant obtained was incubated overnight with proteinase K (0.1 mg/mL) and then with RNase (0.2 mg/mL) for 2 h at 37℃. After extraction with phenol-chloroform (1:1), the DNA was separated in 2% agarose gel and visualized by UV after staining with ethidium bromide. Quantitative assessment of apoptotic cells was assessed by the terminal deoxynucleotidyl transferase-mediated deoxyuridine triphosphate nick endlabeling (TUNEL) method, which examines DNA-strand breaks during apoptosis by using BD ApoAlert™ DNA Fragmentation Assay Kit.

Detection and quantification of acidic vesicular organelles with acridine orange staining

Autophagy is the process of sequestering cytoplasmic proteins into lytic components, and is characterized by the formation and promotion of acidic vesicular organelles (AVO). To assess the occurrence of AVOs, we treated tumor cells with plumbagin for the indicated times then stained them with acridine orange. Briefly,

cells were incubated with acridine orange (1 μg/mL) for 15 minutes, then examined under a fluorescent microscope (5, 11, 24). To quantify the development of AVOs, plumbagin-treated cells were stained with acridine orange (1 μg/mL) for 15 minutes and removed from the plate with trypsin-EDTA. The stained cells were then analysed by means of EPICS flow cytometry (11).

Detection of autophagic vacuoles with monodansylcadaverine

Autophagic vacuoles were also detected with monodansylcadaverine (MDC) by incubating cells with MDC (50 μM) in PBS at 37°C for 10 minutes. After incubation, cells were washed four times with PBS and immediately analyzed by fluorescent microscopy using an inverted microscope (Nikon Eclipse TE 300, Germany) equipped with a filter system (excitation wavelength 380 nm, emission filter 525 nm) (25).

Electron microscopy

Cells or tumor sections were directly fixed with 1% glutaraldehyde and post-fixed with 2% osmium tetroxide. The cell pellets or sections were embedded in epon resin. Representative areas were chosen for ultrathin sectioning and viewed with a JEM 1010 transmission electron microscope (JEOL, Peabody, MA).

Immunoprecipitation/immunoblot, and AKT kinase activity assays

Cells were treated with various concentrations of plumbagin for the indicated times.

For immunoblotting, the cells were lysed on ice for 40 min in a solution containing 50 mM Tris, 1% Triton X-100, 0.1% SDS, 150 mM NaCl, 2 mM Na_3VO_4, 2 mM EGTA, 12 mM β-glycerolphosphate, 10 mM NaF, 16 μg/ml benzamidine hydrochloride, 10 μg/ml phenanthroline, 10 μg/ml aprotinin, 10 μg/ml leupeptin, 10 μg/ml pepstatin, and 1 mM phenylmethylsulfonyl fluoride. The cell lysate was centrifuged at 14,000 × *g* for 15 min, and the supernatant fraction collected for immunoblotting. Equivalent amounts of protein were resolved by SDS-PAGE (10-12%) and transferred to PVDF membranes. After blocking for 1 h in 5% nonfat dry milk in Tris-buffered saline, the membrane was incubated with the desired primary antibody for 1-16 h. The membrane was then treated with appropriate peroxidase-conjugated secondary antibody, and the immunoreactive proteins were detected using an enhanced chemiluminescence kit (Amersham, USA) according to the manufacturer's instructions. AKT activity was determined using kits from Cell Signaling Technology (Beverly, MA) according to the manufacturer's instructions.

Transient transfection of activated AKT-tag cDNA

Transfection of MDA-MB-231 cells was carried out using Lipofectamine 2000 reagent. MDA-MB-231 cells were exposed to the mixture of Lipofectamine 2000 reagent and AKT cDNA plasmid or empty vector with pM1-β-Gal expression vector (Roche) for 6 h. Then, 8 ml of RPMI1640 with 20% FBS was added to each culture

dish. After 18 h of incubation, fresh RPMI1640 was added, and the cells were incubated for another 2 days. Transfection efficiencies were determined by measuring β-galactosidase activity using the β-galactosidase ELISA kit (Roche).

siRNA knockdown of AKT and Beclin-1 expression

Breast cancer cell monolayers were transfected with Beclin-1, AKT1 siRNA duplexes (Sense: GGGCACUUUCGGCAAGGUGtt; antisense: CACCUUGCCGAAAGUGCCCtt) or non-specific control siRNA duplexes (Upstate Biotechnology Inc., NY) by using Lipofectamine 2000 (Invitrogen). Immunoblot analyses showed that Beclin-1 expression was aborted, AKT remained low but detectable, and expression of β-actin was unaffected by siRNA treatment.

In vivo tumor xenograft study

Female nude mice [6 weeks old; BALB/cA-nu (nu/nu)] were purchased from the National Science Council Animal Center (Taipei, Taiwan) and maintained in pathogen-free conditions. MDA-MB-231 cells were injected subcutaneously into the flanks of these nude mice (5×10^6 cells in 200 μl), and tumors were allowed to develop for ~30 days until they reached ~50 mm^3, when treatment was initiated. Twenty mice were randomly divided into two groups. The mice in the plumbagin-treated group were i.p. injected daily with plumbagin in a clear solution containing 25% polyethylene glycol (PEG) (2 mg/kg of body weight) in a volume of 0.2 ml. The

control group was treated with an equal volume of vehicle. After transplantation, tumor size was measured using calipers, and tumor volume was estimated according to the formula: tumor volume (mm^3) = $L \times W^2/2$, where L is the length and W is the width. Tumor-bearing mice were sacrificed after 60 days. Xenograft tumors, as well as other vital organs of the treated and control mice, were harvested and fixed in 4% formalin, embedded in paraffin, and cut into 4-μm sections for histologic study.

Statistical analysis

Data were expressed as means ± SD Statistical comparisons of the results were made using analysis of variance (ANOVA). Significant differences ($p<0.05$) between the means of control and plumbagin-treated cells were analyzed by Dunnett's test.

Results

Plumbagin inhibits cell proliferation and clonogenic survival in MDA-MB-231 and MCF-7 cells

To investigate the potential cell growth inhibition of plumbagin in breast cancer, we first examined the effect of plumbagin on cell proliferation and clonogenic survival in MDA-MB-231 and MCF-7 cells. As shown in Fig. 1A, plumbagin inhibited cell growth in both cancer cell lines in a concentration-dependent manner. The IC_{50} values of plumbagin were 4.4 μM for MDA-MB-231 and 3.2 μM for MCF-7.

Additional experiments were performed to determine the antitumor activities of plumbagin inhibition when analyzed by *in vitro* clonogenic assays. *In vitro* clonogenic assays correlated very well with *in vivo* assays of tumorigenicity in nude mice (26, 27). Fig. 1B and C shows the effects of plumbagin on the relative clonogenicity of the control and the plumbagin-treated MDA-MB-231 and MCF-7 cells. Clonogenicity of both cancer lines was reduced in a concentration-dependent manner after exposure to plumbagin.

Plumbagin induces cell cycle arrest and regulates the expression of cell cycle-related proteins in MDA-MB-231 and MCF-7 cells

To examine the mechanism responsible for plumbagin mediated cell growth inhibition, cell cycle distribution was evaluated using flow cytometric analysis. The results showed that treating cells with plumbagin caused a significant inhibition of cell cycle progression in both cancer cell lines at 6 h (Fig. 2A), resulting in a clear increase in the percentage of cells in the G2/M phase when compared with the control.

Next, we assessed the effects of plumbagin on cell cycle–related regulating factor. Plumbagin treatment of the cells resulted in a time-dependent decrease in the protein expression of cyclinA, cyclinB1, Cdc2 and Cdc25C in both cancer cell lines (Fig. 2B). In addition, exposure of cells to plumbagin for 3 h resulted in an increase in levels of

inactive phospho-Cdc2 (Tyr 15) and phospho-Cdc25C (Ser 216). Exposure of breast cancer cells to 8 μM plumbagin resulted in rapid and sustained activation of Chk2 (phosphorylation at Ser 345). Results from time-dependent studies have indicated that increasing functional Chk2 by increasing phosphorylation was followed by an increase in phospho-Cdc25C, which in turn increased phospho-Cdc2 (Fig. 2B). We suggest that Cdc2 and Cdc25C functions were inhibited by an increase in Chk2 function. Furthermore, the association of p21/WAF1 and Cdc2 increased in a time-dependent manner in plumbagin-treated breast cancer cell lines, as determined by immunoprecipitation assay (Fig. 2C).

Plumbagin does not predominantly induce apoptosis in MDA-MB-231 and MCF-7 cells

Our previous published study showed that plumbagin induces apoptosis in human lung cancer A549 cells (28). At that time, we investigated whether plumbagin could also induce apoptosis in breast cancer. The TUNEL results showed that concentrations of 4 μM and 8μM plumbagin induce only a small amount of apoptotic cell death in MDA-MB-231 and MCF-7 cells after 24 and 48 h treatment (Fig. 3A), whereas treatment of cells with cisplatin (15 μg/mL) for 48 h resulted in an increase in a large amount of DNA breaks in both cell lines. When compared to cisplatin-treated cells, plumbagin treatment also failed to form the “DNA ladder” fragmentation, a typical

marker of apoptosis, detectable by agarose gel electrophoresis at 48 h in MDA-MB-231 and MCF-7 at 4 μM (Fig. 3B).

To verify the possiblility of apoptosis in plumbagin-treated breast cancer cells, we used pan-caspase inhibitor to block caspase activity in both cell lines, and determined whether the cell proliferation inhibition was changed after plumbagin treatment. Blocking caspases activation resulted in a slight decrease in plumbagin-mediated proliferation inhibition in both cell lines, suggesting that plumbagin may induce a small number of breast cancer cells to undergo apoptosis (Fig. 3C).

Plumbagin induces autophagy in MDA-MB-231 and MCF-7 cells

Growing evidence indicates that nonapoptotic programmed cell death is principally attributed to autophagy (type II programmed cell death) (2). The majority of plumbagin-treated breast cancer cells do not primarily display features typical of apoptosis. We next assessed whether plumbagin induces autophagy in breast cancer. As shown in Fig. 4A, plumbagin treatment resulted in the appearance of AVO when cells were stained with acridine orange after 24 h treatment. In addition, bafilomycin, an autophagy inhibitor (29), decreased the accumulation of red fluorescence in both control and plumbagin-treated cells. Because MDC accumulates in mature autophagic vacuoles, such as autophagolysosomes, but not in the early endosome compartment, MDC staining can be used to detect autophagic vacuoles. As shown in Fig. 4A,

treatment of cells with plumbagin increased accumulation of MDC in comparison with the control. These results corroborate the observation that plumbagin treatment induces autophagic cell death in both cancer cell lines.

We also tested whether autophagy occurs in plumbagin-treated cells by using transmission electron microscopy (TEM). The results of TEM showed that in most of the cells, the nuclei maintained their integrity and displayed dispersed chromatin, which is not consistent with an apoptotic character. Normal MDA-MB-231 cells had numerous membrane-bound vesicles, often containing organelles and other cellular fragments (Fig. 4B). In contrast, exposure of cells to 4 and 8 μM plumbagin resulted in the appearance of autophagocytic vacuoles after 12 and 24 h treatment. Autophagocytic vacuoles contained extensively degraded organelles (Fig. 4B). The features of autophagy also revealed in MCF-7 after plumbagin treatment (24 h) (Fig. 4B).

To quantify the accumulation of the acidific component, we performed FACS analysis of acridine orange-stained-cells using the FL3 channel to evaluate the bright red fluorescence, and the FL1 channel to evaluate the green fluorescence (13). As shown in Fig. 4C, plumbagin (8μM) treatment increased the strength of red fluorescence from 3.1% to 19.9% and 1.2% to 18.4% in MDA-MB-231 and MCF-7. In addition, bafilomycin decreased the strength of red fluorescence from 19.9% to

5.4% and 18.4% to 3.3% in 8μM plumbagin treated MDA-MB-231 and MCF-7 cells.

To determine whether the autophagy seen in plumbagin-treated breast cancer cells is involved in cell death, we used siRNA to knockdown Beclin-1 in MDA-MB-231 cells and determine whether autophagy is required for plumbagin-mediated cell proliferation inhibition. Reduction of Beclin-1 (Fig. 4D) resulted in a resistance to plumbagin-mediated proliferation inhibition in MDA-MB-231 cells (Fig. 4E).

Plumbagin inhibits the expression and activity of PI3K/AKT/mTOR pathway

We investigated whether PI3K/AKT/mTOR, which is important in regulating cell proliferation and autophagy, is involved in plumbagin-mediated cell death in both cancer cell lines. Plumbagin treatment of cells was found to cause a significant reduction in the expression of the regulatory subunit of PI3K (p85) protein (Fig. 5A). Similarly, plumbagin caused a significant time-dependent decrease in the phosphorylation (Ser 473 and Thr 308) of AKT protein in cells. Plumbagin treatment did not cause any change in the protein levels of total AKT, however. Exposure of breast cancer cells to plumbagin resulted in diminished levels of the phosphorylated (activated) form of mTOR (Ser 2448 and Ser 2481), a downstream target of PI3K/AKT, which may inhibit cell growth and induce autophagy. Similar responses were observed for the phosphorylated forms of two other AKT downstream targets, GSK-3β (Ser 9) and FKHR (Ser 256). To determine the change of mTOR in

plumbagin-treated MDA-MB-231 and MCF-7 cells, we also examined the phosphorylation of two downstream effectors of mTOR signalin, p70S6K and 4E-BP1. The results showed that phosphorylation levels of both of p70S6K (phospho-p70S6K) and 4E-BP-1 (phospho-4E-BP1) decreased, revealing a potent inhibitory effect of plumbagin on the AKT/mTOR signaling.

Plumbagin-mediated inhibition of AKT was additionally confirmed by determining phosphorylation of one of its substrates, GSK-3α/β. As shown in Fig. 5B, in comparison with the control, the Ser 21/9 phosphorylation of GSK-3α/β decreased after MDA-MB-231 and MCF-7 cells were exposed for 1 h to 8 μM plumbagin. Phosphorylation of GSK-3α/β decreased relative to the control at all 4 time points (Fig. 5B). These results suggest the inhibitory potential of plumbagin against PI3K/AKT pathway, which is highly activated during the development and progression of breast cancer.

The role of AKT pathway in plumbagin-mediated autophagy

Our results show that plumbagin targets the AKT signaling pathway. We next employed genetic inhibition to specifically inhibit AKT to assess the consequences of AKT inhibition on plumbagin-mediated autophagy. To do so, MDA-MB-231 cells were transfected with a pool of siRNA targeting AKT, after which the cells were exposed to 8 μM plumbagin for a specific time. As shown in Fig. 6A, AKT siRNA

reduced AKT expression approximately 60% in comparison with control siRNA. Reduction of AKT expression by transfection of cells with AKT siRNA had no significant effect on MDA-MB-231 autophagy, suggesting that the remaining AKT activity is high enough to maintain survival of the cells. However, treatment with plumbagin increased the number of autophagy cells in AKT siRNA-transfected cells to significantly more than in the control siRNA-transfected cells after 24 h treatment (Fig. 6B and C). This may be due to plumbagin treatment having decreased the level of AKT activity below the threshold for maintaining normal cell survival under these conditions. Thus, this siRNA result further confirms that the AKT signaling pathway is indeed the target of plumbagin treatment.

To confirm the central role of the AKT signaling pathway as a target of plumbagin-induced autophagy, we transfected MDA-MB-231 with a constitutively active form of active AKT cDNA (Fig. 6D). AKT-overexpressing cells were treated with plumbagin, and the induction of autophagy was assayed. Transfected cells expressing active AKT cDNA were considerably more resistant to plumbagin-induced autophagy than cells transfected with the control cDNA. Plumbagin was notably unable to cause autophagy notably in cells transfected with active AKT cDNA, whereas plumbagin could maintain its autophage effects on MDA-MB-231 transfected with the control cDNA (Fig. 6E and F). Therefore, it can be firmly concluded that

plumbagin induces autophagic cell death in MDA-MB-231 by suppression of the AKT pathway.

The role of AKT pathway in plumbagin-mediated cell cycle arrest

To further evaluate the impact of AKT signaling on plumbagin-mediated G2/M arrest, AKT siRNA transfected and AKT-overexpressing MDA-MB-231 cells were exposed to 8 μM plumbagin for a specific time, and the distributions of cell cycle and the expressions of cell cycle-related proteins were assessed. As shown in Fig. 7A, reduction of AKT expression by transfection of cells with AKT siRNA had a slight effect on the cell population at the G2/M phase. However, treatment with plumbagin greatly increased the cell population at the G2/M phase in AKT siRNA-transfected cells to significantly more than in control siRNA and AKT siRNA-transfected cells after 6 h treatment. Decrease of AKT expression by transfection of cells with AKT siRNAs had a slight effect on phosphorylation of Cdc25C, Cdc2 and Chk2, but plumgabin greatly increased the inactive phosphorylation of Cdc25C and Cdc2, and the active phosphorylation of Chk2 when compared with cells transfected with the control and AKT siRNA (Fig. 7B).

On the other hand, transfected cells expressing active AKT cDNA were considerably more resistant to plumbagin mediated G2/M arrest when compared with cells transfected with the control cDNA (Fig. 7C). Furthermore, plumbagin-induced

inactivated phosphorylation of Cdc25C, Cdc2, and activated phosphorylation of Chk2 were significantly prevented by active AKT cDNA transfection in MDA-MB-231 cells (Fig. 7D).

Plumbagin inhibits tumor growth in nude mice

To determine whether plumbagin inhibits tumor growth *in vivo*, equal numbers of MDA-MB-231 cells were injected subcutaneously into both flanks of the nude mice. Tumor growth inhibition was most evident in mice treated with plumbagin at 2 mg/kg/d, where an approximately 70% reduction in tumor size was observed. In contrast with mice treated with the vehicle (Fig. 8A and B). No sign of toxicity, as judged by parallel monitoring of body weight and tissue sections of lungs, livers and kidneys, was observed in plumbagin-treated mice (Fig. 8C). Furthermore, the TEM data also showed an increase of autophagocytic vacuoles in the tumors of the plumbagin-treated mice, when compared to the tumors of vehicle-treated mice (Fig. 8D).

To gain insight into the mechanism of plumbagin's inhibition of tumor growth *in vivo*, we harvested the MDA-MB-231 tumor xenografts from vehicle-treated and plumbagin-treated mice after treatments. We also extracted proteins to assess for levels of PI3K/AKT/mTOR proteins. As shown in Figure 8E, decreases of PI3K (p85) regulatory subunit and phospho-AKT were observed in the tumors of the

plumbagin-treated mice in comparison with tumors of vehicle-treated mice. In addition, the levels of phospho-mTOR were lower in the tumors from the plumbagin-treated group when compared with tumors from vehicle-treated mice.

Discussion

Breast cancer is the most common human neoplasm in both developed and developing countries (30). In our study, we have found that plumbagin effectively inhibits tumor cell growth *in vitro*, concomitant with induction of cell cycle arrest and autophagic cell death, and furthermore inhibits tumor cell growth in nude mice.

In our study, we have found that plumbagin decreases the expression of cyclinB1, cyclinA, Cdc25C, and Cdc2, while it increases the amount of p21/WAF1 and phosphorylation of Cdc2, phospho-Cdc25C and phospho-Chk2. Our results show that plumbagin induces phosphorylation of Cdc25C (Ser 216) through Chk2 activation and remains Cdc25C inactive. Further downstream, inactivated Cdc2 was not dephosphorylated by Cdc25C. Therefore, Cdc2 accumulated in an inactive phosphorylated state (Tyr 15), resulting in cells that were unable to move through the mitotic phase. Furthermore, because the association of p21/WAF1 and Cdc2 also increased in plumbagin-treated MDA-MB-231 and MCF-7 cells, we suggest that plumbagin may prove to be a valuable tool for inhibition of Cdc2/cyclinB1 and

Cdc2/cyclinA complex in breast cancers for the following reasons: (1) the downregulation of plumbagin on cyclinB1 and cyclinA expression, (2) the induction of p21/WAF1 by plumbagin, which may subsequently inhibit the function of Cdc2 by forming Cdc2/p21/WAF complex, and (3) the increase of activated phospho-Chk2 followed by an increase in inactivated phospho-Cdc25C, suggesting that an increase of Chk2 activation follows an increase of Cdc25C, which loses phosphatase function for dephosphorylating and activating Cdc2.

In the present study, we showed that plumbagin induced autophagic cell death but not primarily apoptosis in MDA-MB-231 and MCF-7 cells. Some types of cancer cells exhibit autophagic changes after treatments with irradiation and chemotherapeutic drugs (4, 5, 31). Autophagy begins with the sequestering of cytosolic components, often including intracellular organelles within double-membrane structures. The vacuoles (also called autophagosomes), undergo acidification after maturation. Finally, autophagosomes fuse with lysosomes and their material is digested by lysosomal hydrolases (1, 2). Our results show that the formations of AVOs in MDA-MB-231 cells are characterized by acridine orange and MDC stain after exposures to plumbagin. Moreover, plumbagin-mediated autophagy is blocked by bafilomycin, an autophagy inhibitor. In contrast, the typical characteristic of apoptosis, DNA fragmentation determined by DNA ladder pattern

and TUNEL, is either slight or not observable in plumbagin-treated MDA-MB-231 cells. It is still unclear whether aotophagy suppresses tumorigenesis or provides cancer cells with a protective response under unfavourable conditions, although several studies have reported that autophagy is triggered in cancers, response to various anticancer agents, including As_2O_3, tamoxifen and temozolomide (4, 5, 32, 33). However, whether or not the initiation of different types of cell death is influenced by different stimuli, cell types and cell content requires further investigation.

PI3K/AKT signaling is the major pathway in breast cancer cells and plays a variety of physiologic roles, including cell growth, cell cycle regulation, migration, and survival (8). Activated AKT in turn signals to a variety of key downstream molecules including mTOR, GSK3 and FKHR, the consequence of which is to inhibit cell death and promote cell survival (8). Recent studies have indicated that inhibition of the AKT/mTOR pathway has consistently been associated with triggering autophagy in cancer cells (2, 11-13). Our results show that plumbagin treatment decreases the expression of PI3K p85 regulatory subunit, followed by a decrease of AKT activation and activity. The inhibitory effects of plumbagin on PI3K/AKT are correlated with the loss of phosphorylation of AKT's downstream targets, GSK3 and FKHR. In addition, exposure to plumbagin also inactivated mTOR and reduced phosphorylation of its

downstream targets (p70S6K and 4E-BP1). Moreover, enforced expression of AKT by active AKT cDNA transfection significantly diminished plumbagin-mediated autophagic cell death. In contrast, selective knockdown AKT expression by AKT siRNA-based inhibition increased plumbagin-induced autophagy. Together, these findings indicate that plumbagin induces autophagic cell death through PI3K/AKT/mTOR inhibition in human breast cancer cells.

AKT has been reported to function as a G2/M initiator (34, 35). The AKT activation inhibits initiation of the G2 checkpoint in human cancer cells exposed to radiation and anticancer agents such as cytotoxic methylating agents (35). The suppression mechanism of AKT on G2 arrest is not well-understood, although it has been observed that AKT-mediated G2 checkpoint inhibition is associated with suppression of Chk2 activation and upregulation of cyclinB and Cdc2 expression (34, 35). Furthermore, AKT promotes cell cycle progression at the G2/M transition through Wee1Hu inactivation in mammalian cells (36). In our study, we found that inhibition of AKT was involved in the accumulation of inactive phospho-Cdc2 and phospho-Cdc25C, which may be due to the increase of Chk2 activation, leading to subsequent G2 arrest. These effects, however, were abolished in MDA-MB-231 cells that bear overexpressing AKT cDNA. The present data clearly suggest that the inhibition of AKT pathways plays a role in inducing the G2 checkpoint in

MDA-MB-231 cells following plumbagin exposure.

In conclusion, this study demonstrates that: (*a*) the breast cancer cell line MDA-MB-231 is highly sensitive to growth inhibition by plumbagin both *in vitro* and *in vivo*, (*b*) reduced survival of breast cancer cells after exposure to plumbagin is associated with G2/M phase cell cycle arrest and autophagic cell death, (*c*) plumbagin can inhibit cell cycle progression at the G2/M phase by increasing p21/Cdc2 interaction and Chk2 activation, as well as decreasing the expression of Cdc2, Cdc25C, cyclinB1 and cyclinA, and (*d*) plumbagin-induced autophagic cell death in the human breast cancer cells is mediated by inhibition of the PI3K/AKT/mTOR pathway. Finally, *(e)* it has also been demonstrated that AKT inhibition by plumbagin may also operate in cell cycle arrest by increasing Chk2 activation. These data provide a basic mechanism for the chemotherapeutic properties of plumbagin in breast cancer cells. Future *in vivo* studies using human patients would may ascertain whether this cell growth inhibiton effect of plumbagin might contribute its overall chemotherapy effects in the fight against breast cancer, and possibly have future therapeutic applications.

Acknowledgments

We thank Professor Chun-Ching Lin (Graduate Institute of Natural Products, Kaohsiung Medical University, Kaohsiung, Taiwan) for providing nude mice and

experiment space.

Footnotes

Grant support: National Science Council of Taiwan (NSC 94-2320-B-041-007).

The publication costs of this article were defrayed in part by the payment of page charges. This article must therefore be hereby marked as an advertisement in accordance with 18 U.S.C. Section 1734 to indicate this fact.

References

1. Shintani T, Klionsky DJ. Autophagy in health and disease: a double-edged sword. Science 2004;306:990-5.
2. Kondo Y, Kanzawa T, Sawaya R, Kondo S. The role of autophagy in cancer development and response to therapy. Nat Rev Cancer 2005;5:726-34.
3. Kroemer G, Jaattela M. Lysosomes and autophagy in cell death control. Nat Rev Cancer 2005;5:886-97.
4. Paglin S, Hollister T, Delohery T, et al. A novel response of cancer cells to radiation involves autophagy and formation of acidic vesicles. Cancer Res 2001;61:439-44.
5. Kanzawa T, Kondo Y, Ito H, Kondo S, Germano I. Induction of autophagic cell death in malignant glioma cells by arsenic trioxide. Cancer Res 2003;63:2103-8.
6. Petiot A, Ogier-Denis E, Blommaart EF, Meijer AJ, Codogno P. Distinct classes of phosphatidylinositol 3'-kinases are involved in signaling pathways that control macroautophagy in HT-29 cells. J Biol Chem 2000;275:992-8.
7. Zhao JJ, Gjoerup OV, Subramanian RR, et al. Human mammary epithelial cell transformation through the activation of phosphatidylinositol 3-kinase. Cancer Cell 2003;3:483-95.
8. Hennessy BT, Smith DL, Ram PT, Lu Y, Mills GB. Exploiting the PI3K/AKT

pathway for cancer drug discovery. Nat Rev Drug Discov 2005;4:988-1004.

9. Kraus AC, Ferber I, Bachmann SO, et al. In vitro chemo- and radio-resistance in small cell lung cancer correlates with cell adhesion and constitutive activation of AKT and MAP kinase pathways. Oncogene 2002;21:8683-95.

10. Kirkegaard T, Witton CJ, McGlynn LM, et al. AKT activation predicts outcome in breast cancer patients treated with tamoxifen. J Pathol 2005;207:139-46.

11. Takeuchi H, Kondo Y, Fujiwara K, et al. Synergistic augmentation of rapamycin-induced autophagy in malignant glioma cells by phosphatidylinositol 3-kinase/protein kinase B inhibitors. Cancer Res 2005;65:3336-46.

12. Guertin DA, Sabatini DM. An expanding role for mTOR in cancer. Trends Mol Med 2005;11:353-61.

13. Paglin S, Lee NY, Nakar C, e al. Rapamycin-sensitive pathway regulates mitochondrial membrane potential, autophagy, and survival in irradiated MCF-7 cells. Cancer Res 2005;65:11061-70.

14. Sancar A, Lindsey-Boltz LA, Unsal-Kacmaz K, Linn S. Molecular mechanisms of mammalian DNA repair and the DNA damage checkpoints. Annu Rev Biochem 2004;73:39-85.

15. De Souza CP, Ellem KA, Gabrielli BG. Centrosomal and cytoplasmic Cdc2/cyclin B1 activation precedes nuclear mitotic events. Exp Cell Res

2000;257:11-21.

16. Harvey SL, Charlet A, Haas W, Gygi SP, Kellogg DR. Cdk1-dependent regulation of the mitotic inhibitor Wee1. Cell 2005;122:407-20.

17. Tyagi A, Singh RP, Agarwal C, Siriwardana S, Sclafani RA, Agarwal R. Resveratrol causes Cdc2-tyr15 phosphorylation via ATM/ATR-Chk1/2-Cdc25C pathway as a central mechanism for S phase arrest in human ovarian carcinoma Ovcar-3 cells. Carcinogenesis 2005;26:1978-87.

18. Mossa JS, El-Feraly FS, Muhammad I. Antimycobacterial constituents from Juniperus procera, Ferula communis and Plumbago zeylanica and their in vitro synergistic activity with isonicotinic acid hydrazide. Phytother Res 2004;18:934-7.

19. Srinivas P, Gopinath G, Banerji A, Dinakar A, Srinivas G. Plumbagin induces reactive oxygen species, which mediate apoptosis in human cervical cancer cells. Mol Carcinog 2003;40:201-11.

20. Tilak JC, Adhikari S, Devasagayam TP. Antioxidant properties of Plumbago zeylanica, an Indian medicinal plant and its active ingredient, plumbagin. Redox Rep 2004;9:219-27.

21. Ding Y, Chen ZJ, Liu S, Che D, Vetter M, Chang CH. Inhibition of Nox-4 activity by plumbagin, a plant-derived bioactive naphthoquinone. J Pharm

Pharmacol 2005;57:111-6.

22. Sugie S, Okamoto K, Rahman KM, et al. Inhibitory effects of plumbagin and juglone on azoxymethane-induced intestinal carcinogenesis in rats. Cancer Lett 1998;127:177-83.

23. Hazra B, Sarkar R, Bhattacharyya S, Ghosh PK, Chel G, Dinda B. Synthesis of plumbagin derivatives and their inhibitory activities against Ehrlich ascites carcinoma in vivo and Leishmania donovani Promastigotes in vitro. Phytother Res 2002;16:133-7.

24. Shao Y, Gao Z, Marks PA, Jiang X. Apoptotic and autophagic cell death induced by histone deacetylase inhibitors. Proc Natl Acad Sci U.S.A 2004;101:18030-5.

25. Munafo DB, Colombo MI. A novel assay to study autophagy: regulation of autophagosome vacuole size by amino acid deprivation. J Cell Sci 2001;114:3619-29.

26. Freedman VH, Shin SI. Cellular tumorigenicity in nude mice: correlation with cell growth in semi-solid medium. Cell 1974;3:355-9.

27. Shin SI, Freedman VH, Risser R, Pollack R. Tumorigenicity of virus-transformed cells in nude mice is correlated specifically with anchorage independent growth in vitro. Proc Natl Acad Sci U.S.A 1975;72:4435-4439.

28. Hsu YL, Cho CY, Kuo PL, Huang YT, Lin CC. Plumbagin

(5-Hydroxy-2-methyl-1,4-naphthoquinone) Induces Apoptosis and Cell Cycle Arrest in A549 Cells through p53 Accumulation via c-Jun NH2-Terminal Kinase-Mediated Phosphorylation at Serine 15 in Vitro and in Vivo. J Pharmacol Exp Ther 2006;318:484-94.

29. Yamamoto A, Tagawa Y, Yoshimori T, Moriyama Y, Masaki R, Tashiro, Y. Bafilomycin A1 prevents maturation of autophagic vacuoles by inhibiting fusion between autophagosomes and lysosomes in rat hepatoma cell line, H-4-II-E cells. Cell Struct Funct 1998;23:33-42.
30. Paik S. Molecular profiling of breast cancer. Curr Opin Obstet Gynecol 2006;18:59-63.
31. Ellington AA, Berhow MA, Singletary KW. Inhibition of Akt signaling and enhanced ERK1/2 activity are involved in induction of macroautophagy by triterpenoid B-group soyasaponins in colon cancer cells. Carcinogenesis 2006;27: 298-306.
32. Bilir A, Altinoz MA, Erkan M, Ozmen V, Aydiner, A. Autophagy and nuclear changes in FM3A breast tumor cells after epirubicin, medroxyprogesterone and tamoxifen treatment in vitro. Pathobiology 2001;69:120-6.
33. Kanzawa T, Germano IM, Komata T, Ito H, Kondo Y, Kondo S. Role of autophagy in temozolomide-induced cytotoxicity for malignant glioma cells.

Cell Death Differ 2004;11:448-57.

34. Liang J, Slingerland JM. Multiple roles of the PI3K/PKB (Akt) pathway in cell cycle progression. Cell Cycle 2003;2:339-45.

35. Hirose Y, Katayama M, Mirzoeva OK, Berger MS, Pieper RO. Akt activation suppresses Chk2-mediated, methylating agent-induced G2 arrest and protects from temozolomide-induced mitotic catastrophe and cellular senescence. Cancer Res 2005;65:4861-9.

36. Katayama K, Fujita N, Tsuruo T. Akt/protein kinase B-dependent phosphorylation and inactivation of WEE1Hu promote cell cycle progression at G2/M transition. Mol Cell Biol 2005;25:5725-37.

Figure Legends

Fig. 1. The inhibiting effects of plumbagin on cell proliferation and colony formation in MDA-MB-231 and MCF-7. (A) Inhibition effect of plumbagin on cell proliferation in MDA-MB-231 and MCF-7. (B) Influence of breast cancer cells on the number of colony-forming cells, as evaluated by clonogenic assay. (C) Representative dishes by colony-forming assay. For (A), cell growth inhibition activity of plumbagin was assessed by XTT. For colony-forming assay, the clonogenic assay was performed as described in Materials and Methods. Each value is the mean ± SD of three determinations. Results shown are representative of three independent experiments. The asterisk indicates a significant difference between control and plumbagin-treated cells, * $p<0.05$.

Fig. 2. Plumbagin induces cell cycle arrest and regulates the expression of cell cycle-related proteins in MDA-MB-231 and MCF-7 cells. (A) The distribution of cell cycles in plumbagin-treated cells. (B) The effect of plumbagin in cell cycle-related proteins. (C) The effect of plumbagin on association of p21/WAF1 and Cdc2. For (A), cells were treated with vehicle and plumbagin for 6 h, and cell cycle distribution was assessed by flow cytometry. For (B), the cell cycle-related expression levels of 8 μM plumbagin-treated cancer cells were determined by Western blotting. For (C), cell lysates were subjected to immunoprecipitation with anti-Cdc2, followed by immunoblotting analysis with anti-p21/WAF1. Results shown are representative of

three independent experiments. The asterisk indicates a significant difference between control and plumbagin-treated cells, * $p<0.05$.

Fig. 3. The effect of plumbagin on apoptosis induction in breast cancer cells. Plumbagin induce only small amount of apoptosis in both cells lines, as determined by TUNEL (A) and agarose gel electrophoresis (B). (C) The effect of z-VAD-FMK on plumbagin-mediated cell proliferation inhibition. For (A), cells were treated with various concentrations of plumbagin and cisplatin for the indicated times, and then stained by ApoAlert™ DNA Fragmentation Assay Kit. The TUNEL-positive cells were examined by flow cytometry. For (B), DNA fragmentation was assessed by agarose gel electrophoresis. For (C), cells were treated with z-VAD-FMK (20 μM) for 1 h, and then 8 μM plumbagin was added and incubated for 48 h. Cell proliferation was assessed by XTT. Results shown are representative of three independent experiments. The asterisk indicates a significant difference between control and plumbagin-treated cells, * $p<0.05$.

Fig. 4. Plumbagin induces autophagic cell death in two human breast cancer cells. (A) plumbagin-treated cells were stained with acridine orange and MDC. (B) The appearances of autophagocytic vacuoles were examined by transmission electron microscopy. Numerous autophagic vacuoles (*arrows*) and empty vacuoles (*arrowheads*) were observed. (C) The quantification of acridine orange staining using

flow cytometry. (D) The inhibition of Beclin-1 expression by siRNA transfection. (E) The effect of reducing Beclin-1 siRNA on plumbagin-mediated cell proliferation inhibition. Results shown are representative of three independent experiments. The asterisk indicates a significant difference between control and plumbagin-treated cells, * $p<0.05$.

Fig. 5. Plumbagin inhibits the expression and activity of PI3K/AKT/mTOR pathway. (A) The effect of plumbagin on the levels of PI3K, AKT, GSK, FKHR, mTOR, p70S6K, 4E-BP1 and their phosphorylated form. (B) The effect of plumbagin on AKT activity. For (A), the cells were treated with 8 μM plumbagin at different times. The control cells received an equal volume of DMSO. The cell lysates were prepared, and Western blotting was performed using antibodies against various PI3K/AKT/mTOR and phospho-AKT/mTOR signaling proteins. For (B), the AKT kinase activity was determined using an AKT assay activity kit from Cell Signaling Technology (Beverly, MA) according to the manufacturer's instructions. Results shown are representative of three independent experiments.

Fig. 6. The role of AKT inhibition in plumbagin-mediated autophagic cell death. (A) Genetic suppression of AKT by AKT siRNA transfection. (B) The induction of autophagy of plumbagin in control and AKT siRNA transfected cells. (C) The quantification of acridine orange staining using flow cytometry. (D) Overexpression

of AKT by active AKT cDNA transfection. (E) The induction of autophagy of plumbagin in AKT cDNA transfected cells. (F) The quantification of acridine orange staining using flow cytometry. MDA-MB-231 cells were transfected with control oligonucleotide, AKT siRNA, control-cDNA or active AKT cDNA, then treated with plumbagin for the indicated times. The degree of autophagic cell death was assessed by acridine orange and MDC stain. Results shown are representative of three independent experiments. The asterisk indicates a significant difference between control and plumbagin-treated cells, * $p<0.05$.

Fig. 7. The role of AKT inhibition in plumbagin-mediated cell cycle arrest. (A) The influence of AKT inhibition by siRNA in plumbagin-mediated G2/M arrest (B) The expression of Chk2 and phospho-Chk2 in siRNA transfected cells treated with or without plumbagin. (C) The influence of AKT overexpression by active AKT cDNA transfection in plumbagin-mediated G2/M arrest. (D) The expression of Chk2 and phospho-Chk2 in AKT cDNA transfected cells treated with or without plumbagin. MDA-MB-231 cells were transfected with control oligonucleotide, AKT siRNA, control-cDNA or active AKT cDNA, then treated with plumbagin for the indicated times (3 h for cell cycle-related proteins, 6 h for cell cycle analysis). The expressions of various proteins were assessed by Western blotting analysis. Cell cycle distribution was determined by flow cytometry analysis. The asterisk indicates a significant

difference between control and plumbagin-treated cells, * $p<0.05$.

Fig. 8. Plumbagin inhibits growth of MDA-MB-231 in nude mice. (A) Representative tumor-possessing nude mice and tumors from the control and plumbagin-treated groups. (B) Mean of tumor volume measured at the indicated number of days after implant. (C) Tissue sections of livers, lungs, and kidneys of plumbagin-treated nude mice determined by H&E stain. (D) Plumbagin induced autophagic cell death in the tumors of nude mice, as determined by TEM. Numerous autophagic vacuoles (*arrows*) and empty vacuoles (*arrowheads*) were observed. (E) Plumbagin inhibits the expression levels of PI3K/AKT/mTOR signaling protein in MDA-MB-231 xenograft. Animals bearing pre-established tumors (n = 15 per group) were dosed daily for 60 days with i.p. injections of plumbagin (2mg/kg/d) or vehicle. During the 60-day treatment, tumor volumes were estimated using measurements taken by external calipers (mm^3). The levels of various PI3K/AKT/mTOR signaling proteins were assessed by immunoblot analysis. Each value is the mean ± SD of three determinations.

A.

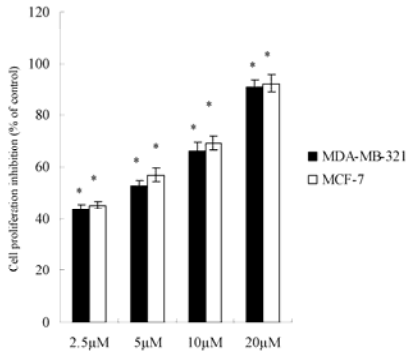
120
100
80
60
40
20
0
Cell proliferation inhibition (% of control)
MDA-MB-321
MCF-7
2.5μM
5μM
10μM
20μM

B.

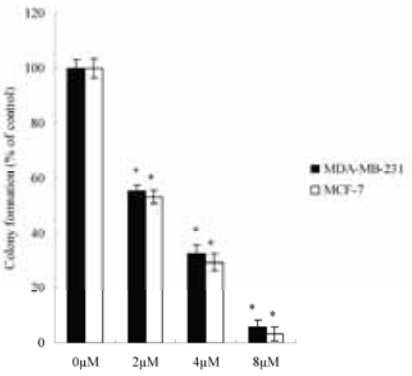
120
100
80
60
40
20
0
Colony formation (% of control)
MDA-MB-231
MCF-7
0μM
2μM
4μM
8μM

C.

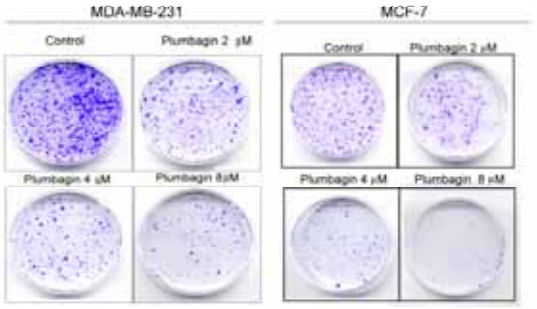
MDA-MB-231
MCF-7
Control
Plumbagin 2 μM
Control
Plumbagin 2 μM
Plumbagin 4 μM
Plumbagin 8μM
Plumbagin 4 μM
Plumbagin 8 μM

Figure 1.

A.

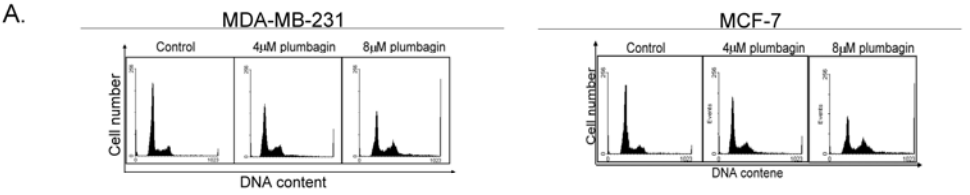

MDA-MB-231	G0/G1(%)	S (%)	G2/M(%)
Control	74.3± 2.4	11.7±0.5	14.0±2.1
Plumbagin 4 μM	62.4± 2.1*	12.1±0.7	25.5+1.9*
Plumbagin 8 μM	58.5± 1.9*	11.6±1.0	29.9±2.1*

MCF-7	G0/G1(%)	S (%)	G2/M(%)
Control	78.3± 1.9	10.5±0.6	11.2±2.3
Plumbagin 4 μM	63.6± 2.1*	13.1±0.8	23.3+2.1*
Plumbagin 8 μM	51.4± 2.2*	11.3±1.4	37.3±2.6*

B.

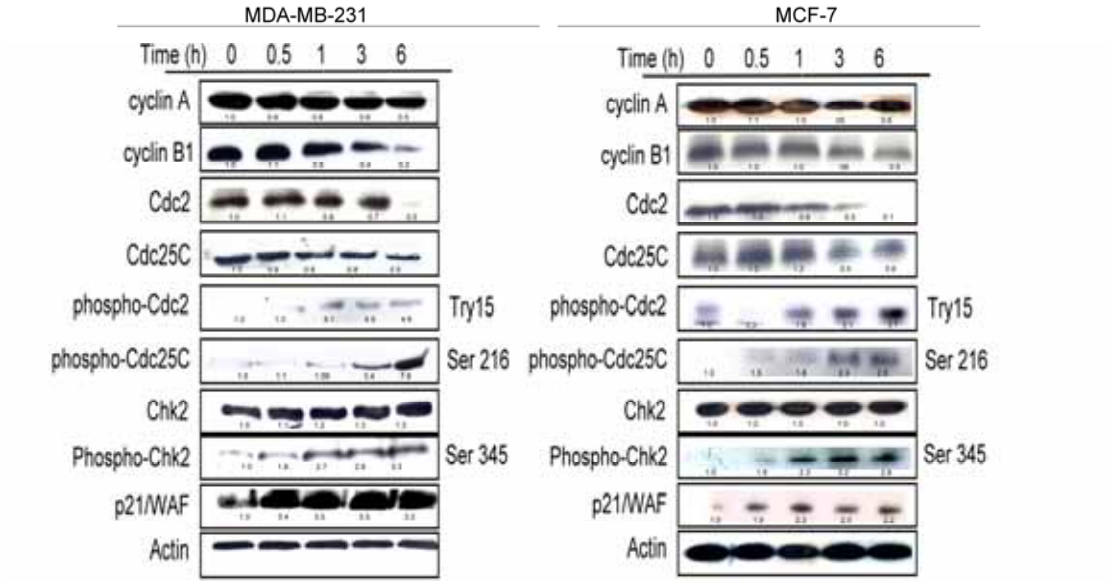

C.

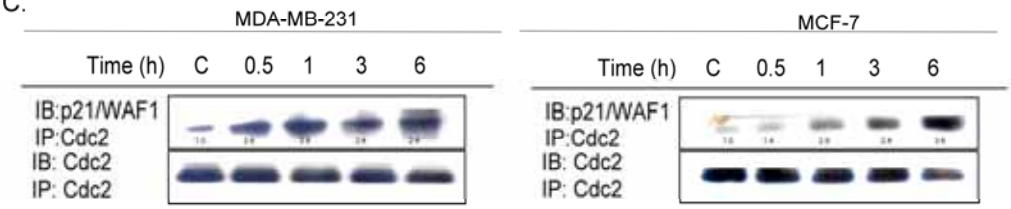

Figure 2.

A.

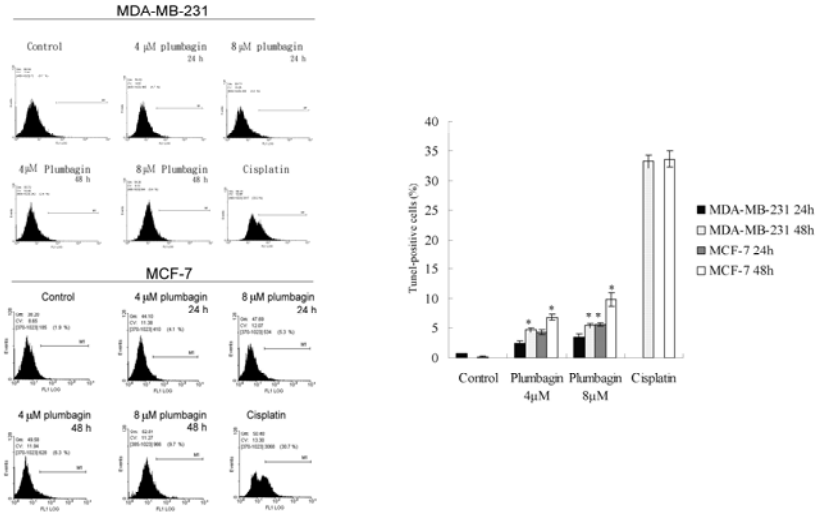
MDA-MB-231
Control
4 μM plumbagin 24 h
8 μM plumbagin 24 h
4μM Plumbagin 48 h
8μM Plumbagin 48 h
Cisplatin
MCF-7
Control
4 μM plumbagin 24 h
8 μM plumbagin 24 h
4 μM plumbagin 48 h
8 μM plumbagin 48 h
Cisplatin
Tunel-positive cells (%)
MDA-MB-231 24h
MDA-MB-231 48h
MCF-7 24h
MCF-7 48h
Control
Plumbagin 4μM
Plumbagin 8μM
Cisplatin

B.

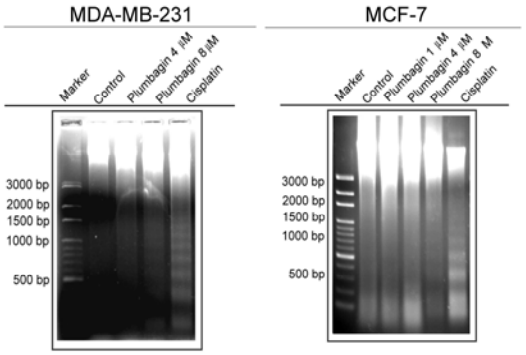
MDA-MB-231
Marker
Control
Plumbagin 4 μM
Plumbagin 8 μM
Cisplatin
3000 bp
2000 bp
1500 bp
1000 bp
500 bp
MCF-7
Marker
Control
Plumbagin 1 μM
Plumbagin 4 μM
Plumbagin 8 μM
Cisplatin
3000 bp
2000 bp
1500 bp
1000 bp
500 bp

C.

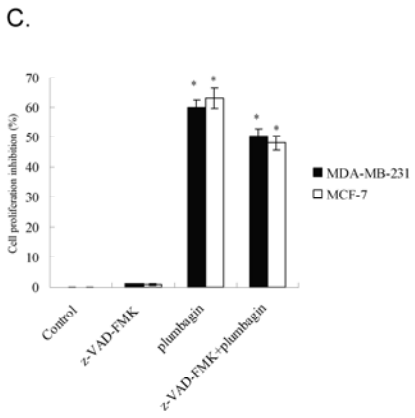
Cell proliferation inhibition (%)
MDA-MB-231
MCF-7
Control
z-VAD-FMK
plumbagin
z-VAD-FMK+plumbagin

Figure 3.

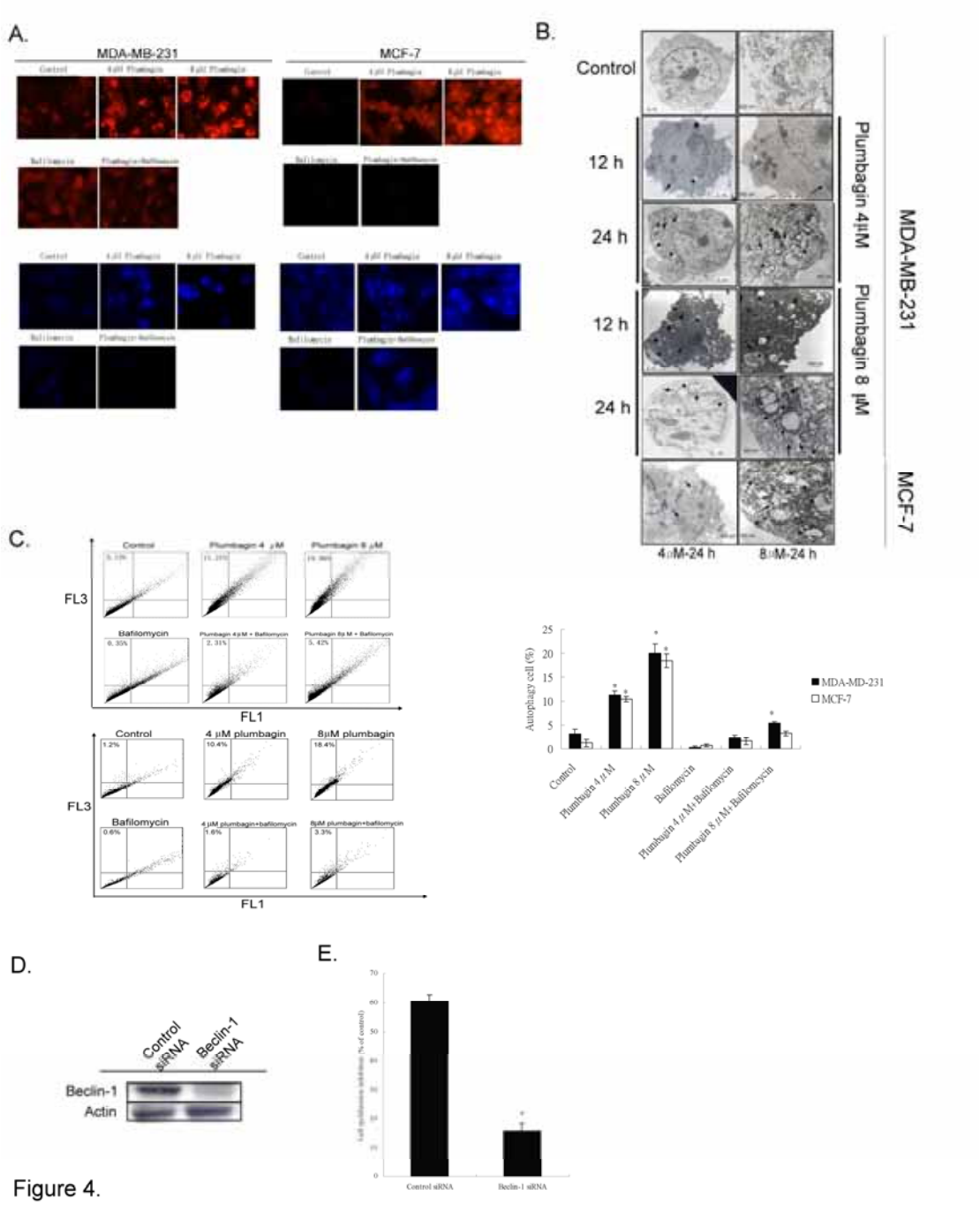
A.
MDA-MB-231
MCF-7
B.
Control
12 h
24 h
12 h
24 h
Plumbagin 4μM
Plumbagin 8 μM
MDA-MB-231
MCF-7
4μM-24 h
8μM-24 h
C.
Control
Plumbagin 4 μM
Plumbagin 8 μM
FL3
Bafilomycin
FL1
4 μM plumbagin
8μM plumbagin
Autophagy cell (%)
MDA-MD-231
MCF-7
Control
Plumbagin 4 μM
Plumbagin 8 μM
Bafilomycin
Plumbagin 4 μM+Bafilomycin
Plumbagin 8 μM+Bafilomycin
D.
Control siRNA
Beclin-1 siRNA
Beclin-1
Actin
E.
Control siRNA
Beclin-1 siRNA

Figure 4.

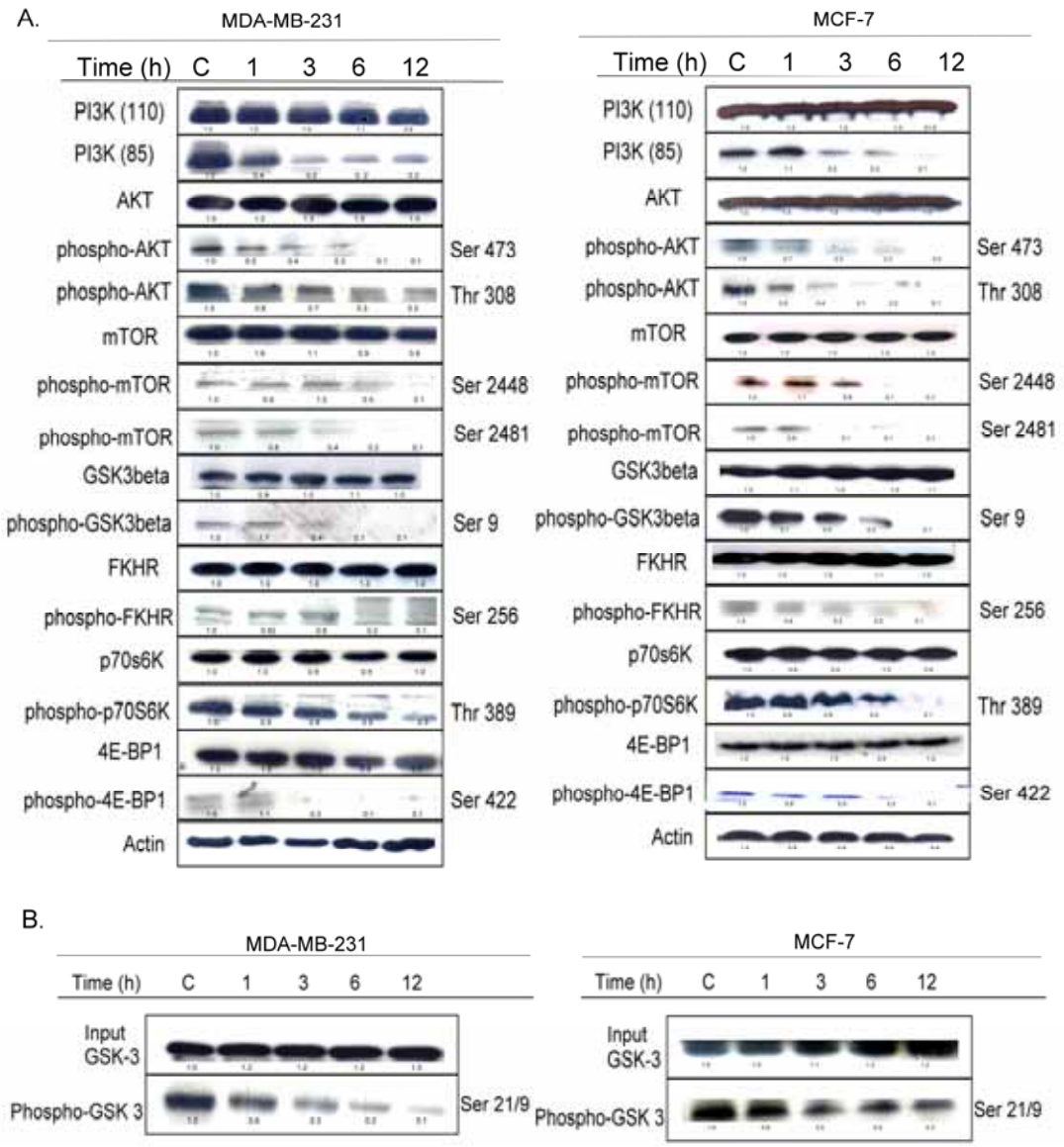
A.
MDA-MB-231
MCF-7
Time (h) C 1 3 6 12
PI3K (110)
PI3K (85)
AKT
phospho-AKT
Ser 473
phospho-AKT
Thr 308
mTOR
phospho-mTOR
Ser 2448
phospho-mTOR
Ser 2481
GSK3beta
phospho-GSK3beta
Ser 9
FKHR
phospho-FKHR
Ser 256
p70s6K
phospho-p70S6K
Thr 389
4E-BP1
phospho-4E-BP1
Ser 422
Actin
B.
MDA-MB-231
MCF-7
Time (h) C 1 3 6 12
Input GSK-3
Phospho-GSK 3
Ser 21/9

Figure 5.

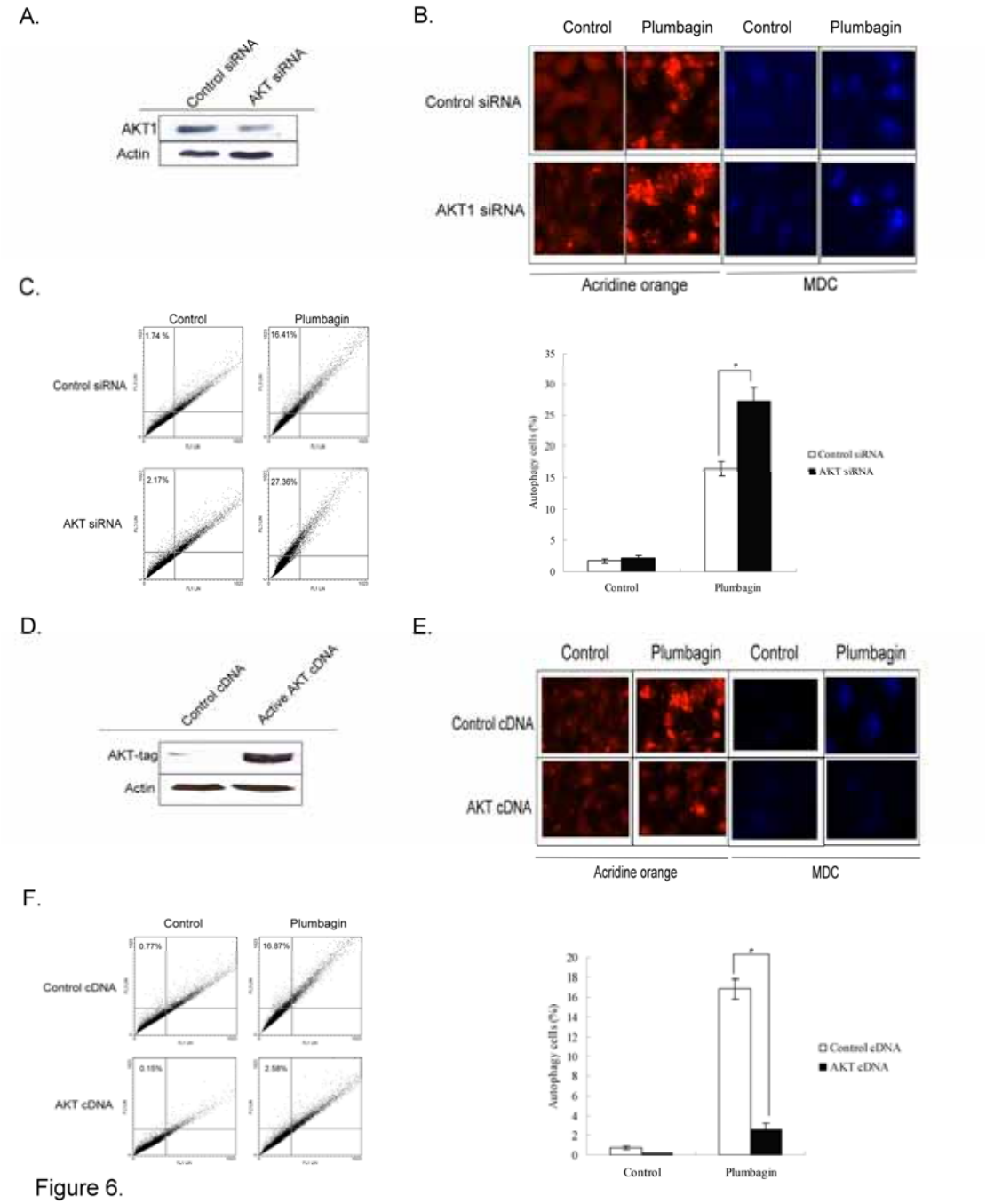
A.
Control siRNA
AKT siRNA
AKT1
Actin
B.
Control
Plumbagin
Control
Plumbagin
Control siRNA
AKT1 siRNA
Acridine orange
MDC
C.
Control
Plumbagin
Control siRNA
AKT siRNA
1.74 %
16.41%
2.17%
27.36%
Autophagy cells (%)
Control siRNA
AKT siRNA
Control
Plumbagin
D.
Control cDNA
Active AKT cDNA
AKT-tag
Actin
E.
Control
Plumbagin
Control
Plumbagin
Control cDNA
AKT cDNA
Acridine orange
MDC
F.
Control
Plumbagin
Control cDNA
AKT cDNA
0.77%
16.87%
0.18%
2.58%
Autophagy cells (%)
Control cDNA
AKT cDNA
Control
Plumbagin

Figure 6.

A.

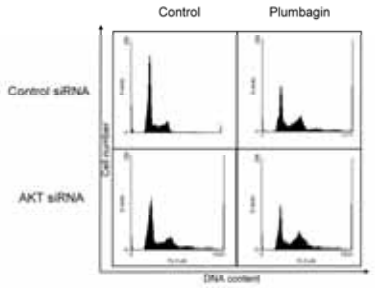

		G0/G1(%)	S(%)	G2/M(%)
control siRNA	Control	74.6±1.3	11.9±0.7	13.5±1.1
	Plumbagin	61.2±1.6*	11.6±0.8	27.2±1.3*
AKT siRNA	Control	66.3±1.5	13.6±0.7	20.1±1.3
	Plumbagin	51.2±1.4*	11.4±0.8	37.4±1.2*

B.

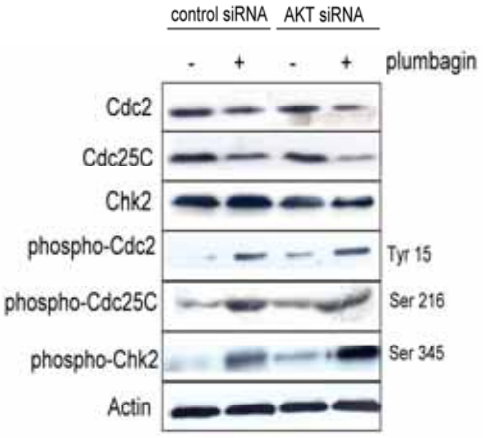

C.

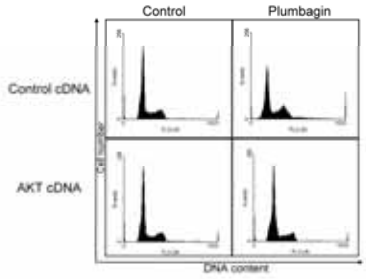

		G0/G1(%)	S(%)	G2/M(%)
control cDNA	Control	73.9±1.6	12.8±0.6	13.3±1.9
	Plumbagin	62.9±1.6*	12.4±0.7	24.7±1.8*
AKT cDNA	Control	76.1±1.4	11.3±0.6	12.6±1.5
	Plumbagin	74.9±1.8	12.5±0.5	12.6±1.4

D.

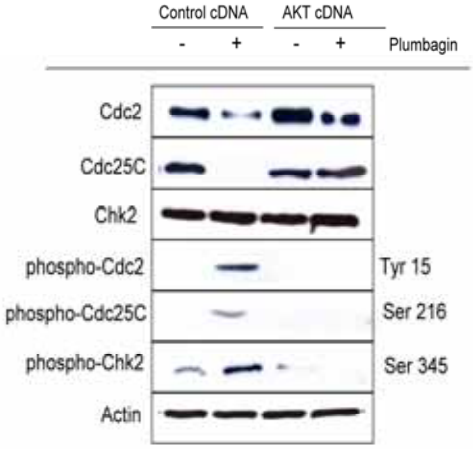

Figure 7.

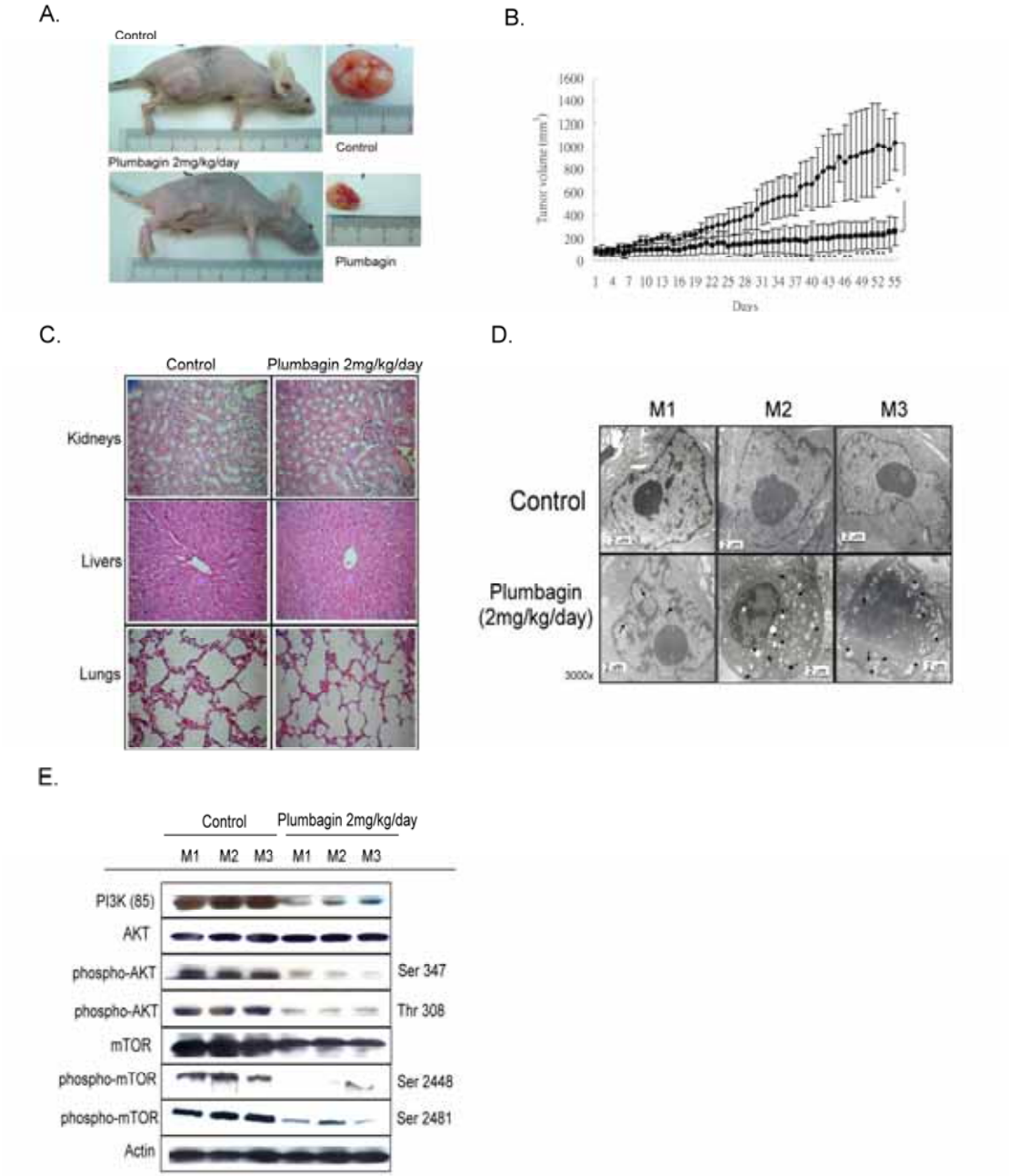
A.
Control
Control
Plumbagin 2mg/kg/day
Plumbagin
B.
Tumor volume (mm³)
1600
1400
1200
1000
800
600
400
200
0
1 4 7 10 13 16 19 22 25 28 31 34 37 40 43 46 49 52 55
Days
C.
Control
Plumbagin 2mg/kg/day
Kidneys
Livers
Lungs
D.
M1
M2
M3
Control
Plumbagin
(2mg/kg/day)
3000x
E.
Control
Plumbagin 2mg/kg/day
M1 M2 M3 M1 M2 M3
PI3K (85)
AKT
phospho-AKT
Ser 347
phospho-AKT
Thr 308
mTOR
phospho-mTOR
Ser 2448
phospho-mTOR
Ser 2481
Actin

Figure 8.